Enhanced Exciton Harvesting in a Planar Heterojunction Organic Photovoltaic Device by Solvent Vapor Annealing

Yiwei Zhang[1], Muhammad T. Sajjad[1], Oskar Blaszczyk[1], Arvydas Ruseckas[1], Luis A Serrano[2], Graeme Cooke[2], and Ifor D. W. Samuel[1]*

1.Organic Semiconductor Centre, SUPA, School of Physics and Astronomy, University of St Andrews, North Haugh, St Andrews, KY16 9SS, UK

2.Glasgow Centre for Physical Organic Chemistry, WESTCHEM, School of Chemistry, University of Glasgow, Glasgow G12 8QQ, UK

E-mail: idws@st-andrews.ac.uk

ABSTRACT: The singlet exciton diffusion length was measured in a small molecule electron donor material DR3TBDTT using fluorescence quenching at a planar interface with a cross-linked fullerene derivative. The one-dimensional exciton diffusion length was increased from 16 to 24 nm by annealing the film in carbon disulfide solvent vapor. Planar heterojunction solar cells were fabricated using bilayers of these materials and it was found that solvent vapor annealing increased the short circuit current density by 46%. This can be explained by improved exciton harvesting in the annealed bilayer.

KEYWORDS: organic solar cells, exciton diffusion length, photoluminescence quenching, bilayer

1.Introduction

Organic photovoltaics (OPVs) are a promising solar technology that has attracted considerable research interest.[1-5] OPVs have some attractive features compared to silicon based PVs, including solution processability, compatibility with large area and flexible substrates, low weight and low cost. In OPV devices, the generation of photocurrent starts from the absorption of photons in the active layer, which leads to the formation of bound electron-hole pairs (known as excitons); to split excitons into charges, energy is needed to overcome the Coulomb potential. The energy difference between donor and acceptor lowest unoccupied molecular orbital (LUMO) levels can provide the energy needed. In this scenario, to undergo dissociation into charge pairs the excitons need to travel to the donor-acceptor interface during their lifetime. The average distance an exciton can diffuse within its lifetime known as the exciton diffusion length (L_D), and is usually much shorter than the absorption length.[6-9]

The simplest OPV structure is the planar heterojunction device, which consists of a planar donor layer and a planar acceptor layer in contact with each other.[10] The excitons diffuse within the film and some of them can reach the donor-acceptor interface where dissociation occurs, and charges are generated, which then move to the contacts and provide the photocurrent. Only the excitons that can diffuse to the donor-acceptor interface contribute to charge generation and hence photocurrent. Therefore, in planar heterojunction OPV devices, the diffusion length determines the useful thickness of the light absorbing layer that contributes to photocurrent generation. Due to the limited exciton diffusion length in organic semiconducting materials, the efficiency of bilayer OPV devices is generally much lower than bulk heterojunction devices. However, planar heterojunction cells would offer simpler large-scale production and better long-term stability. Exciton harvesting in planar heterojunction devices can be improved by increasing exciton diffusion length [11] and introducing additional light-harvesting layers with long-range energy transfer.[12] Most of the bi-layer OPV devices are fabricated using orthogonal solvent strategy that still allows some inter-diffusion of the donor and acceptor molecules and formation of

a mixed heterojunction layer at the boundary [13, 14]. In that case it is difficult to separate the processing effects on exciton harvesting and charge separation.

In this work we investigated the effect of solvent vapour annealing (SVA) on exciton harvesting and solar cell performance in a bilayer of a small molecule electron donor material DR3TBDTT and a cross-linked fullerene derivative, [6,6]-phenyl-C_{61}-butyric acid styryl dendron ester (PCBSD) (molecular structures are shown in Figure 1). This method provided a well-defined planar donor-acceptor interface without inter-diffusion. We found that annealing using a low boiling point non-halide solvent, carbon disulfide (CS_2) increased the exciton diffusion length in DR3TBDTT which lead to an enhancement in short circuit current (J_{sc}) in planar heterojunction OPV. The operation of the devices was analysed using a simple optical model, and it was found that the J_{sc} improvement observed upon SVA was due to increased exciton diffusion length. The improved exciton diffusion length upon SVA is the main reason for the higher device power conversion efficiency (*PCE*).

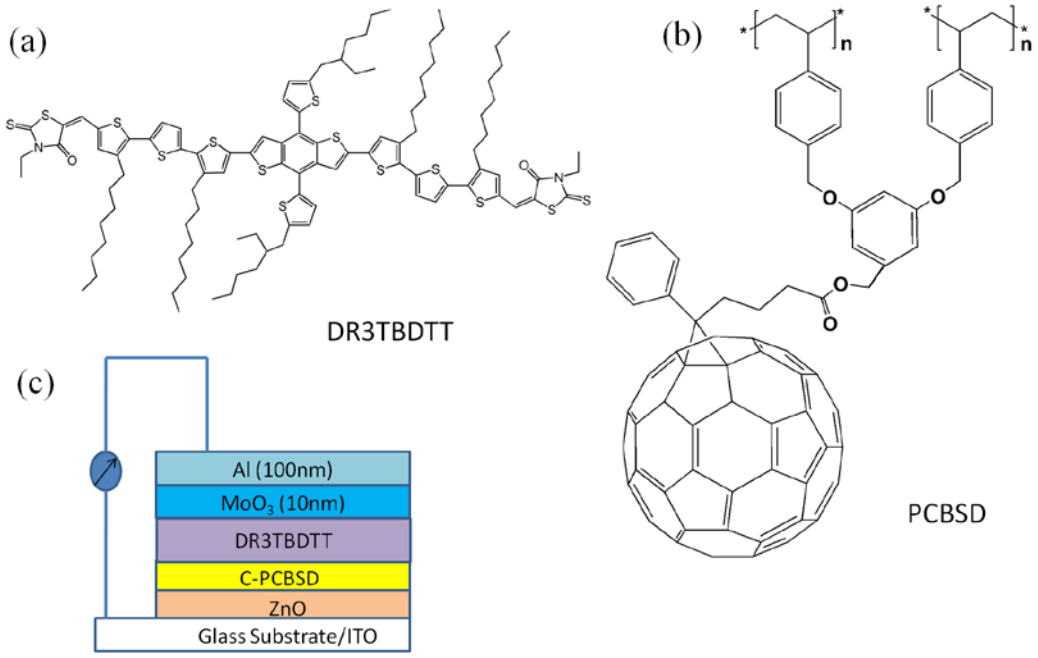

Figure 1. Molecular structure of (a) DR3TBDTT and (b) PCBSD. (c) Structure of the bilayer device used in this work.

2. *Material and methods*

DR3TBDTT was purchased from 1-Material. This molecule was previously used to make bulk heterojunction solar cells [15, 16]. We employed time-resolved measurements of photoluminescence surface quenching to measure exciton diffusion. For this experiment PCBSD was synthesized as previously described and used as the quenching layer [17]. The PCBSD layer was spin-coated from a dichlorobenzene solution, and the films were then annealed at 170 ^{o}C for 40 minutes to realise polymerization. The resulting films were rinsed by chlorobenzene to remove any unpolymerized material. DR3TBDTT was then spin-coated from a chloroform solution. We fabricated two films for each film thickness: one was on a cross-linked PCBSD quenching layer, and the other one was on a fused silica substrate. A range of thicknesses were made by adjusting spin-coating speed and solution concentration. The SVA treatment was conducted by pipetting 200 μL of CS_2 through the edges of a glass petri dish (diameter was 10 cm) and the DR3TBDTT films were kept inside for 45 seconds with the lid closed. All the sample preparation was conducted inside a nitrogen-filled glove box and the samples were transferred to a testing chamber without exposure to air. The absorption spectra were measured using a Cary 300 UV-Vis spectrophotometer. Time-resolved fluorescence measurements were conducted in vacuum. The samples were excited using 200 fs light pulses at 515 nm with 80 MHz repetition rate and fluorescence was detected using a Hamamatsu synchroscan streak camera.

We fabricated planar heterojunction OPV devices using an inverted structure of ITO/ZnO (35 nm)/PCBSD (20 nm)/DR3TBDTT (30 nm) /MoO_3 (10 nm)/Al (100 nm), as shown in Figure 1(c). Here the zinc oxide electron transport layer was fabricated using a sol-gel [18] method and processed in air. The PCBSD and DR3TBDTT layers were prepared in the same way as the films used for surface quenching samples. MoO_3 and Al were evaporated through a shadow mask by a thermal evaporator under a vacuum of 2×10^{-6} mbar. The devices were finished by encapsulating them using

UV-cured epoxy glue and a glass cover slip. The photovoltaic properties were characterised by illuminating with a Sciencetech solar simulator and measuring JV properties with a Keithley 2400 source-measure unit. The irradiance was calibrated using a silicon detector and a KG-5 filter. The external quantum efficiency (*EQE*) was measured by exposing the device to monochromatic light supplied from a Xenon arc lamp and a monochromator.

3. Results and discussion

As can be seen in Figure 2(a) the absorption coefficient of DR3TBDTT film is slightly enhanced by SVA, which we attribute to the molecules in the film orienting closer to parallel to the substrate. The photoluminescence spectra showed no obvious shift after SVA. The roughness of the film was measured by atomic force microscope (AFM) over an area of 1 μm^2 and found to decrease from 4.1 to 3.0 nm after SVA. (See Figure S1) The absorption coefficient of PCBSD layer before and after SVA is shown in Figure 2(b). Absorption mainly occurs at wavelengths shorter than 500 nm and almost did not change upon SVA.

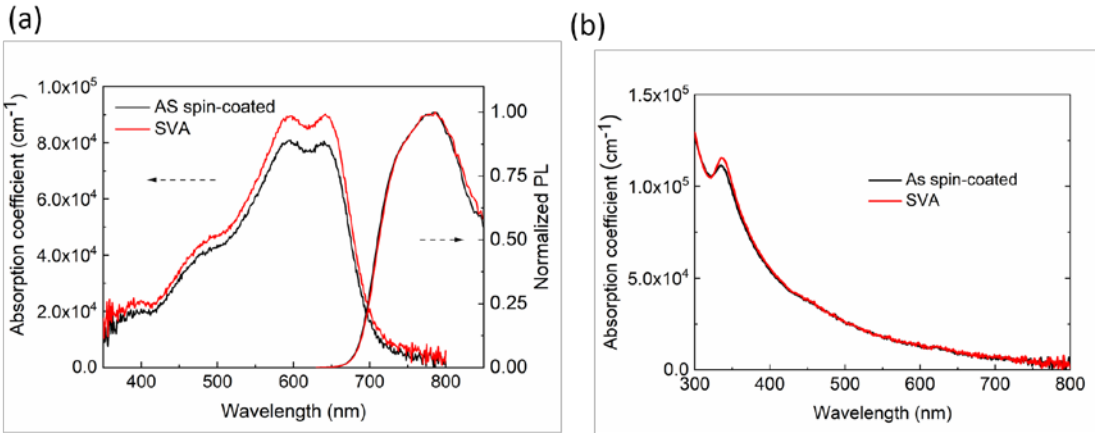

Figure 2. (a) Absorption coefficient / photoluminescence spectra of DR3TBDTT films and (b) absorption coefficient of PCBSD films with and without SVA.

Fluorescence decays of DR3TBDTT films on top of quencher (PCBSD) and on non-quenching fused silica substrate are shown in Figure 3. We observe faster

quenching in thinner DR3TBDTT films because excitons diffuse a shorter distance to the quenching surface. Exciton diffusion can be described by the diffusion equation: [19, 20]

$$\frac{\partial n}{\partial t} = D\frac{\partial^2 n}{\partial x^2} - k(t)n - k_F n + G(x) \quad (1)$$

where n is the exciton density, D is the diffusion coefficient, $k(t)$ is the decay rate of excitons, k_F is quenching rate due to Förster resonance energy transfer (FRET) to the quencher, $G(x)$ is the exciton generation rate as a function of position.

In the present study, to solve the diffusion equation, the instantaneous generation assumption was applied as our excitation light pulse is short; and no FRET is considered as the absorption wavelength of PCBSD is much shorter than the emission of DR3TBDTT.[21] For the PL quenching at the DR3TBDTT/PCBSD interface, a boundary condition of $n|_{x=0} = 0$ was applied; which means no exciton exists at the fullerene quencher surface and we assumed that no quenching occurs at the top surface, which gave the second boundary condition of $\partial n / \partial x|_{x=d} = 0$, where d is the thickness of the DR3TBDTT film. By fitting the fluorescence decay of the reference sample and solving the diffusion equation numerically under the assumptions presented above, the additional decay due to exciton diffusion to the quenching layer can be obtained. For all the three thicknesses, the experimental data were fitted globally with the diffusion coefficient as the only parameter. We obtained the diffusion coefficient of $(1.5 \pm 0.2) \times 10^{-3}$ $cm^2 s^{-1}$ in the as-spin-coated samples, whilst for CS_2 SVA treated samples, the diffusion coefficient increased to $(3.5 \pm 0.5) \times 10^{-3}$ $cm^2 s^{-1}$, which is more than double the diffusion coefficient of films without CS_2 SVA treatment.

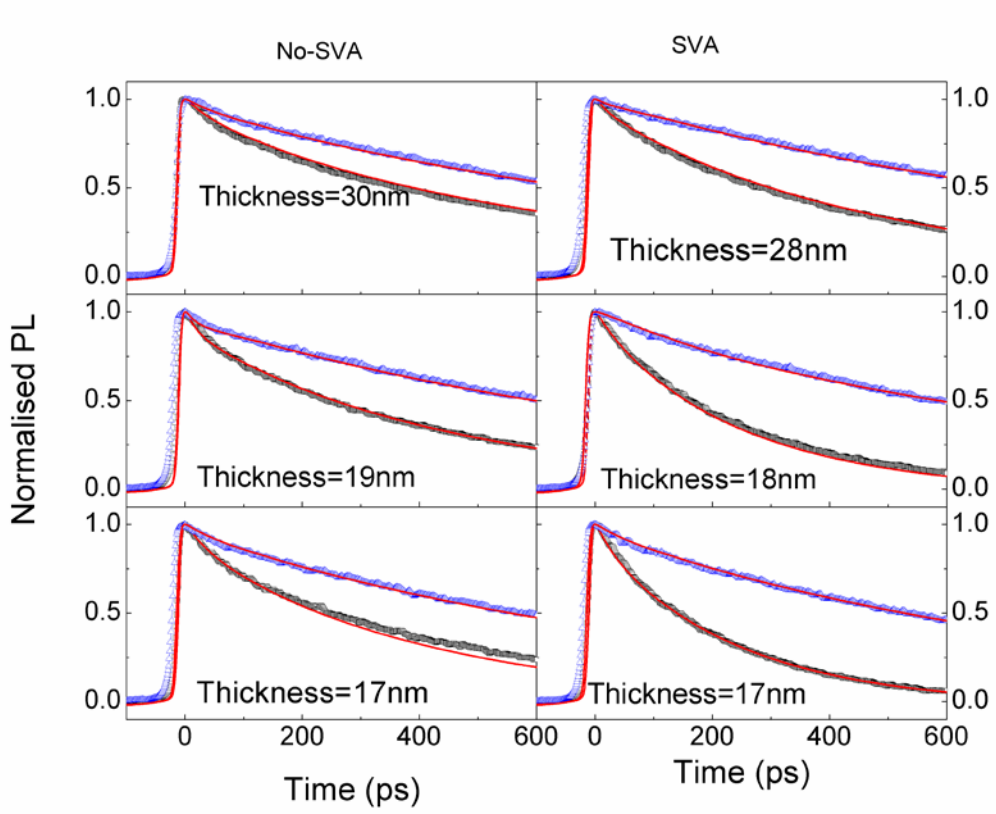

Figure 3. Photoluminescence decays for three thicknesses of DR3TBDTT films on fused silica (blue dots) and PCBSD substrates (black dots). Solid lines represent fits to the data with the diffusion equation (Equation 2). After SVA, the quenching at the PCBSD surface was enhanced which is reflected by faster PL decay of DR3TBDTT films on PCBSD compared to the untreated counterparts.

In the case of one-dimensional diffusion, the diffusion length can be obtained from $L_D = \sqrt{2D\tau}$,[7, 22] where τ is the lifetime of the exciton and can be obtained from the PL decay measurement of neat films. We took the time decay to 1/e of its initial intensity as the lifetime, being (840 ± 10) and (850 ± 10) ps for as spin-coated and solvent vapor annealed films respectively, indicating that SVA does not significantly affect the PL decay. The exciton diffusion length in as spin-coated and SVA treated samples were determined to be (15.7 ± 1.0) nm and (24.3 ± 1.7) nm respectively.

We have considered possible reasons for the increase in exciton diffusion length.

It has been shown theoretically that [23] the exciton diffusion length increases with the photoluminescence quantum yield (PLQY) and decreases with the refractive index. However, in our case, the PLQY showed only a slight decrease upon SVA from 5.9% to 5.8%, and the index of refraction determined from ellipsometry measurements only increased very slightly, as shown in Figure S2. As the changes in PLQY and refractive index are very small, they cannot account for the large change in exciton diffusion length.

A more likely explanation for the increase in exciton diffusion length is a change in the film morphology. We explored this using atomic force microscopy (AFM) and found that the crystallite size increases after SVA. This is further supported by previous XRD observation, [16] in which SVA led to difference in the (100) diffraction peak indicating different crystallite structure due to different tilting angles of alkyl chains. Hence, we consider that the increase in exciton diffusion length after SVA is likely due to the molecules packing after SVA is favourable for exciton diffusion.

As shown in Figure 4 and Table 1, the *PCE* of the bilayer device was enhanced from 0.57% to 0.98% upon CS_2 SVA. The enhancement of *PCE* can be attributed to an improvement in J_{sc}, which increased from 2.4 to 3.5 mA/cm^2 after SVA, and an enhancement in *FF* from 0.36 to 0.43. The enhancement in J_{sc} can also be seen from the external quantum efficiency (*EQE*), as shown in Figure 4(b), the peak value of *EQE* increased from 15.3% for the untreated devices to 22.1% for the solvent vapor annealed devices.

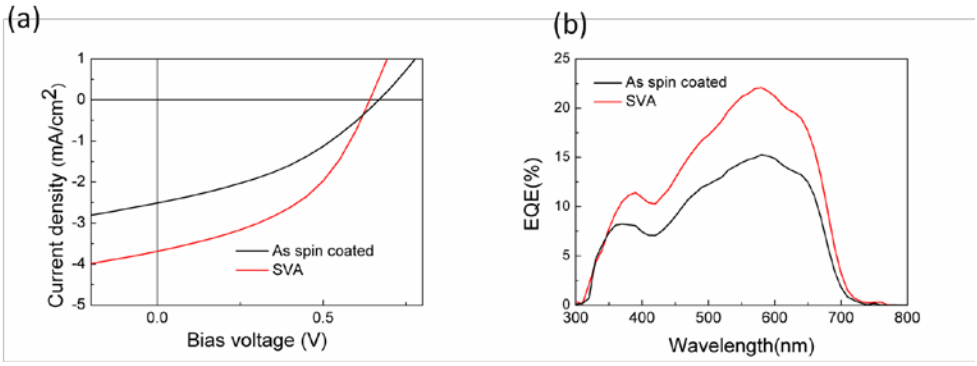

Figure 4. J-V curves (a) and EQE (b) of bilayer planar heterojunction devices with/without CS_2 SVA.

Table 1 Device performance before and after solvent vapor annealing with CS_2.

Device type	PCE (%)	V_{oc} (V)	FF	J_{sc} (mA/cm^2)	Peak EQE (%)
As spin-coated	0.64 (0.57±0.05)*	0.67 (0.65±0.01)	0.38 (0.36±0.019)	2.5 (2.4±0.07)	15.3
CS_2 SVA	1.1 (0.98±0.04)	0.64 (0.64±0.01)	0.45 (0.43±0.013)	3.7 (3.5±0.11)	22.1

*The values in the brackets are the average and standard deviation of 8 devices.

We calculated the electric field distribution through the bilayer OPV device structure as a function of position using the transfer matrix method. [24-26] The distribution of the optical field is shown in Figure S3. The exciton generation density is proportional to the squared electrical field strength and can be determined accordingly, which is shown in Figure S4.

In this scenario, the photocurrent originates from the flux of excitons diffusing to the donor/acceptor interface, it can be expressed as:

$$j = e\eta D \frac{\partial n(x)}{\partial x}\Big|_{x=d} \quad (2)$$

Here, η is the charge collection efficiency, *e* is charge on an electron and *d* is the thickness of DR3TBDTT film.

We then solve the diffusion equation (Equation (1)) at steady state taking the exciton generation into consideration. The steady state diffusion equation can be expressed as:

$$G(x) = D(\frac{1}{L_D^{\ 2}} - \frac{\partial^2}{\partial x^2})n(x) \quad (3)$$

Here we choose a parabolic format to fitting the exciton generation profile, which has been used by Siegmund et al. [27] and it is reasonable in our case, supporting by the shape of optical field distribution in Figure S3 and good fitting

quality in Figure S4. The exciton generation can be expressed as:

$$G(x) = ax^2 + bx + c \quad (4)$$

Applying the boundary conditions of complete exciton quenching at the DR3TBDTT/PCBSD interface and complete exciton reflection at the DR3TBDTT/MoO_3 interface, the diffusion equation can be solved analytically. Hence the resulting current density (j) can be written as:[27]

$$j = e\eta L_D \left[\tanh\frac{d}{L_D}(G(d) + 2aL_D{}^2) + bL_D\left(\frac{1}{\cosh\frac{d}{L_D}} - 1\right) - 2adL_D \right] \quad (5)$$

Here, η is assumed to be 100%. According to Equation (5) and the exciton generation profile in our case, the current density for bilayer devices can be plotted versus the exciton diffusion length, as shown in Figure 5. The photo current density for bilayer devices with/without SVA in this study were indicated in Figure 5.

The model predicts an increase of the photo current density in the bilayer device structure by increasing the exciton diffusion length. For the measured values of L_D the current density enhancement predicted by the model was ~40%, which is close to the experimental results (J_{sc} enhanced by ~46%). Therefore, the increased J_{sc} and *EQE* in solvent vapor annealed devices is mainly or entirely caused by the enhanced exciton diffusion length. A further benefit of SVA is that it enhances the *FF* from 0.36 to 0.43, which also contribute to the *PCE* of the bilayer devices.

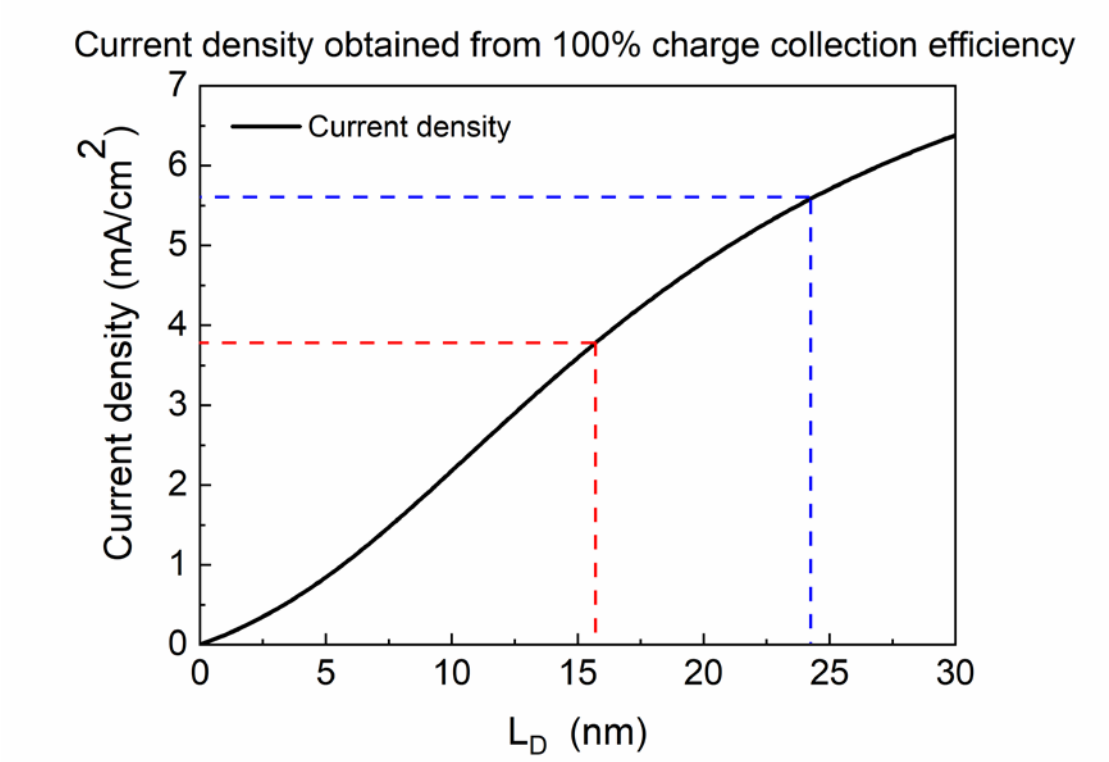

Figure 5. Calculated short circuit current as a function of exciton diffusion length of DR3TBDTT. The red and blue dashed lines indicate the exciton diffusion length of DR3TBDTT films before and after solvent vapor annealing.

4.Conclusion

In summary, we explored the effect of SVA treatment using CS_2 in a highly efficient small molecule donor material. We observed an enhancement (more than two times) in exciton diffusion coefficient, leading to a 46% increase in exciton diffusion length upon SVA. We then fabricated bilayer heterojunction OPV devices and observed the enhancement in J_{sc} and *PCE*. From the calculation based on an optical model, the enhanced exciton diffusion length was found to be the main reason for the better device performance. These results indicate that exciton diffusion length is directly related to the exciton harvesting and device performance of planar heterojunction OPV devices.

Acknowledgement:

We thank the European Research Council (ERC) for financial support (EXCITON grant 321305). Data supporting this study is available at DOI:10.17630/0e75f92d-6f8a-41be-ad45-ac6d1d890ee2.

References:

[1] L. Dou, J. You, Z. Hong, Z. Xu, G. Li, R.A. Street, Y. Yang, 25th Anniversary Article: A Decade of Organic/Polymeric Photovoltaic Research, Adv Mater, 25 (2013) 6642-6671.

[2] A.J. Heeger, 25th Anniversary Article: Bulk Heterojunction Solar Cells: Understanding the Mechanism of Operation, Adv Mater, 26 (2014) 10-28.

[3] S. Li, L. Ye, W. Zhao, S. Zhang, S. Mukherjee, H. Ade, J. Hou, Energy-Level Modulation of Small-Molecule Electron Acceptors to Achieve over 12% Efficiency in Polymer Solar Cells, Adv Mater, 28 (2016) 9423-9429.

[4] J. Hou, O. Inganäs, R.H. Friend, F. Gao, Organic solar cells based on non-fullerene acceptors, Nature Materials, 17 (2018) 119-128.

[5] L. Lu, T. Zheng, Q. Wu, A.M. Schneider, D. Zhao, L. Yu, Recent Advances in Bulk Heterojunction Polymer Solar Cells, Chemical Reviews, 115 (2015) 12666-12731.

[6] E. Shaw Paul, A. Ruseckas, D.W. Samuel Ifor, Exciton Diffusion Measurements in Poly(3‐hexylthiophene), Adv Mater, 20 (2008) 3516-3520.

[7] O.V. Mikhnenko, P.W.M. Blom, T.-Q. Nguyen, Exciton diffusion in organic semiconductors, Energy & Environmental Science, 8 (2015) 1867-1888.

[8] S.M. Menke, R.J. Holmes, Exciton diffusion in organic photovoltaic cells, Energy & Environmental Science, 7 (2014) 499-512.

[9] G.J. Hedley, A. Ruseckas, I.D.W. Samuel, Light Harvesting for Organic Photovoltaics, Chemical Reviews, 117 (2017) 796-837.

[10] C.W. Tang, Two‐layer organic photovoltaic cell, Applied Physics Letters, 48 (1986) 183-185.

[11] S.M. Menke, W.A. Luhman, R.J. Holmes, Tailored exciton diffusion in organic photovoltaic cells for enhanced power conversion efficiency, Nature Materials, 12 (2012) 152.

[12] K. Cnops, B.P. Rand, D. Cheyns, B. Verreet, M.A. Empl, P. Heremans, 8.4% efficient fullerene-free organic solar cells exploiting long-range exciton energy transfer, Nature Communications, 5 (2014) 3406.

[13] H. Li, Z.-G. Zhang, Y. Li, J. Wang, Tunable open-circuit voltage in ternary organic solar cells, Applied Physics Letters, 101 (2012) 163302.

[14] H. Li, Y.-F. Li, J. Wang, Optimizing performance of layer-by-layer processed polymer solar cells, Applied Physics Letters, 101 (2012) 033907.

[15] J. Zhou, Y. Zuo, X. Wan, G. Long, Q. Zhang, W. Ni, Y. Liu, Z. Li, G. He, C. Li, B. Kan, M. Li, Y. Chen, Solution-Processed and High-Performance Organic Solar Cells Using Small Molecules with a Benzodithiophene Unit, J Am Chem Soc, 135 (2013) 8484-8487.

[16] M. Li, F. Liu, X. Wan, W. Ni, B. Kan, H. Feng, Q. Zhang, X. Yang, Y. Wang, Y. Zhang, Y. Shen, T.P.

Russell, Y. Chen, Subtle Balance Between Length Scale of Phase Separation and Domain Purification in Small-Molecule Bulk-Heterojunction Blends under Solvent Vapor Treatment, Adv Mater, 27 (2015) 6296-6302.
[17] Y. Long, G.J. Hedley, A. Ruseckas, M. Chowdhury, T. Roland, L.A. Serrano, G. Cooke, I.D.W. Samuel, Effect of Annealing on Exciton Diffusion in a High Performance Small Molecule Organic Photovoltaic Material, Acs Appl Mater Inter, 9 (2017) 14945-14952.
[18] T. Yang, W. Cai, D. Qin, E. Wang, L. Lan, X. Gong, J. Peng, Y. Cao, Solution-Processed Zinc Oxide Thin Film as a Buffer Layer for Polymer Solar Cells with an Inverted Device Structure, The Journal of Physical Chemistry C, 114 (2010) 6849-6853.
[19] S.R. Scully, M.D. McGehee, Effects of optical interference and energy transfer on exciton diffusion length measurements in organic semiconductors, J Appl Phys, 100 (2006) 034907.
[20] A.J. Ward, A. Ruseckas, I.D.W. Samuel, A Shift from Diffusion Assisted to Energy Transfer Controlled Fluorescence Quenching in Polymer–Fullerene Photovoltaic Blends, The Journal of Physical Chemistry C, 116 (2012) 23931-23937.
[21] C.-H. Hsieh, Y.-J. Cheng, P.-J. Li, C.-H. Chen, M. Dubosc, R.-M. Liang, C.-S. Hsu, Highly Efficient and Stable Inverted Polymer Solar Cells Integrated with a Cross-Linked Fullerene Material as an Interlayer, J Am Chem Soc, 132 (2010) 4887-4893.
[22] M.T. Sajjad, A.J. Ward, C. Kästner, A. Ruseckas, H. Hoppe, I.D.W. Samuel, Controlling Exciton Diffusion and Fullerene Distribution in Photovoltaic Blends by Side Chain Modification, The Journal of Physical Chemistry Letters, 6 (2015) 3054-3060.
[23] D. Yeboah, J. Singh, Dependence of Exciton Diffusion Length and Diffusion Coefficient on Photophysical Parameters in Bulk Heterojunction Organic Solar Cells, Journal of Electronic Materials, 46 (2017) 6451-6460.
[24] G.F. Burkhard, E.T. Hoke, M.D. McGehee, Accounting for Interference, Scattering, and Electrode Absorption to Make Accurate Internal Quantum Efficiency Measurements in Organic and Other Thin Solar Cells, Adv Mater, 22 (2010) 3293-3297.
[25] L.A.A. Pettersson, L.S. Roman, O. Inganäs, Modeling photocurrent action spectra of photovoltaic devices based on organic thin films, J Appl Phys, 86 (1999) 487-496.
[26] P. Peumans, A. Yakimov, S.R. Forrest, Small molecular weight organic thin-film photodetectors and solar cells, J Appl Phys, 93 (2003) 3693-3723.
[27] B. Siegmund, M.T. Sajjad, J. Widmer, D. Ray, C. Koerner, M. Riede, K. Leo, I.D.W. Samuel, K. Vandewal, Exciton Diffusion Length and Charge Extraction Yield in Organic Bilayer Solar Cells, Advanced Materials, 29 (2017) 1604424.